Materials
Views
www.MaterialsViews.com

ADVANCED
MATERIALS
INTERFACES
www.advmatinterfaces.de

Sensitive Humidity-Driven Reversible and Bidirectional Bending of Nanocellulose Thin Films as Bio-Inspired Actuation

Miao Wang, Xuelin Tian,* Robin H. A. Ras, and Olli Ikkala*

Inspired by plant movements caused by water swelling and deswelling within nano- and mesoscale cellulose fibrillar structures, asymmetric exposure of water vapors to thin films of nanofibrillated cellulose, NFC (also denoted as microfibrillated cellulose, MFC, or native cellulose nanofibers, CNF) is here shown to induce humidity-controlled reversible actuation. The extent of the bending depends on the humidity difference across the film. A steady-state bending is reached within a fraction of minute upon continued humidity exposure, and the film relaxes back upon removing the imposed humidity. The bending curvature becomes reduced when the film thickness increases, thus explaining that the effect is not observable in classic paper sheets, which are much thicker due to their constituent macroscopic thicker cellulose fibers. The bending is highly sensitive to humidity, as demonstrated by the observation that the film bends even based on the small humidity of human hand from a distance of several millimeters. Such a bending of a cellulose nanofiber film offers a particularly simple route toward biomimetic actuation and novel types of active material.

1. Introduction

Biological materials and organisms provide a rich source of inspiration for materials scientists to understand how structural design at the nano- and mesoscale can be employed to achieve attractive functional properties in the macroscale.[1] Biomimetic materials have dealt with tunable and responsive mechanical properties,[2] structural colors,[3] and wetting.[4] Toward actuation and movement, the biological machinery[5] allows subtle de novo approaches but in several cases simpler systems are sought, where the movements can be triggered by simple stimuli, such as magnetic or electric field,[6] pH,[7] temperature,[8] light,[9] humidity,[10] or electrochemically.[11] Also, surfaces with actuating "hairs" have been shown,[12] inspired by biological cilia and flagella, as well as actuating gels.[13] In plants, movements and bendings take place based on various mechanisms, for example, asymmetric cell growth, turgor pressure, and water swelling and deswelling within the structures.[14] A particular example of the latter concept concerns pine cones, where asymmetrically positioned differently aligned layers of the nano- and mesoscale cellulose fibrils induce asymmetric water swelling, leading to bending.[15] In this way, the structure can be considered to be a biological counterpart to so-called bilayer actuators, which are extensively used in technology and science, involving different expansions of the two layers upon temperature or other signals.[8a,c,11c,e,14e,16]

The above plant-based actuation inspired us to investigate water swelling/deswelling-dependent bending in films consisting of nanofibrillated cellulose (commonly denoted as NFC (nanofibrillated cellulose), MFC (microfibrillated cellulose), or CNF (cellulose nanofibers)), i.e., native cellulose nanofibers. NFC has high tensile stiffness and strength,[17] but due to their nanometer scale lateral dimensions they allow facile bending. On the other hand, previously it has been observed that upon placing a classic paper sheet on the surface of liquid water, it starts to bend, as water penetrates into the sheet from below and initiates asymmetric swelling.[18] Thus, a "bilayer" is formed based on the bottom hydrated swollen layer and the upper more dry layer. However, when the water front reaches the sheet upper surface, the asymmetry is suppressed and the paper sheet recovers its original flat shape. It has to be noticed that classic papers are relatively thick due to their microscopic cellulose constituent fibers, thus providing relatively high flexural stiffness. Here, our initial hypothesis was that if we use NFC instead of classic thick pulp fibers of high bending stiffness, we could achieve more sensitive actuation, even to allow triggering by water vapors, as the nanoscopic NFC fibers allow facile bending and making thinner sheets than those of classic paper.

In the following, we describe that sufficiently thin NFC-based films show highly sensitive and bidirectional water-vapor-triggered bending (**Figure 1**) to allow even complex bent shapes. The phenomena will be demonstrated first qualitatively and then quantitatively.

M. Wang, Dr. X. Tian, Prof. R. H. A. Ras, Prof. O. Ikkala
Department of Applied Physics
Aalto University, P. O. Box 15100
FI-00076 Espoo, Finland
E-mail: Xuelin.Tian@aalto.fi; Olli.Ikkala@aalto.fi

2. Results and Discussion

The films were prepared by filtration of aqueous dispersion of NFC, followed by drying under ambient conditions (see the
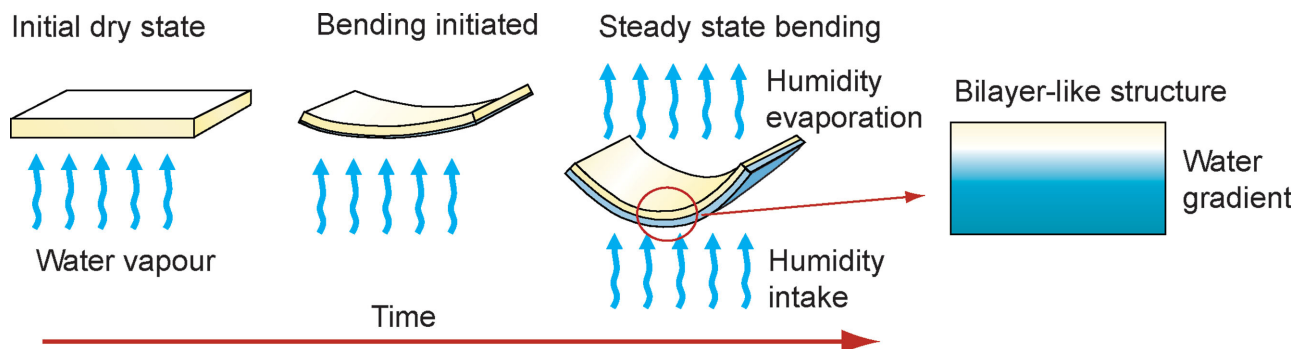
Figure 1. Schematics of a water vapor-based actuation in nanofibrillated cellulose (NFC) films of thickness in the range of 10 μm. The bending reaches a humidity and thickness-dependent steady-state value, unlike in asymmetrically wetted classic paper sheets, where the bending is transient (see Figure S1, Supporting Information), as terminated when the water front penetrates throughout the paper sheet.[18]

Experimental Section). The thickness of the NFC films was controlled by adjusting the volume of aqueous dispersion during the filtration process, and disc-shaped films of a diameter of 3.6 cm with a typical thickness of 8 μm were used in most of our studies unless otherwise mentioned. Thicker films were made to study the bending as a function of the films thickness. Morphology of the NFC film was investigated by scanning electron microscopy (Supporting Information, Figure S2), which indicated a random dense network structure and no obvious preferential in-plane fibril orientation as observed from the top.

A qualitative first indication that the films behave in a surprising way is observed by holding a thin NFC film on a bare hand, where the film spontaneously starts to bend upward in a few seconds (Figure 1, **Figure 2**a). The bending increases until it seems to acquire a steady-state value in tens of seconds. Importantly, it does not relax back even upon holding the film on the hand for prolonged times. However, the film recovers its original flat shape in tens of seconds when moving away from the hand, indicating that the bending is reversible. On the other hand, if the bent film on the hand was turned upside down, it becomes flat again and further continues to bend in the reverse direction (Figure 2b). The reversible and bidirectional deflection processes take roughly tens of seconds and are more clearly illustrated in Supplementary Movie 1 (Supporting Information). The movement depends on the direction of the stimulus; therefore, the actuation can be denoted as tropic.[19]

The above qualitative observations indicate that a thin 8-μm NFC film sensitively senses the presence of uncovered human skin, due to either the small temperature or the humidity gradient. Next, we put a flat NFC film at the open door of a hot oven with its surface parallel to the door. In this case, the film did not bend at all, suggesting that the actuation is not driven by a temperature gradient. To qualitatively verify the role of humidity, we put the flat NFC film on a latex glove-covered hand, whereupon no deflection was observed (Figure S3, Supporting Information). Obviously, the glove acted as a humidity barrier between the skin and the film. Therefore, the higher humidity close to a bare hand should be responsible for the actuation. This is not surprising as the physiochemical property of the NFC is important for the high moisture sensitivity of the film. As a hydrophilic polymeric material, NFC has numerous hydroxyl and oxygen-containing groups along the high surface area of the nanofibers, which makes it highly sensitive to

humidity change and able to absorb moisture even from very dilute water vapor environment.

Next, quantitative measurements were undertaken to shed light on the mechanism and to understand how to control the actuation. We employed a home-made humidity chamber (Figure S4, Supporting Information), where the internal relative humidity (RH) can be adjusted from 10% to in excess of 50%. The exterior of the chamber (i.e., the ambient room) has a constant RH of about 10% ± 4%. On the wall of the humidity chamber, there was a window of a diameter ≈3.6 cm (Figure S5, Supporting Information), with a removable cover lid that could be opened to position a film instead. Positioning the film there allowed to impose a well-controlled relative humidity difference (ΔRH) across the NFC film. The bending of the film was monitored using a video camera, and the curvature k (cm^{-1}) was calculated as described in the Experimental Section (also Supporting Information, Figure S5 for illustration). We first investigated the effect of ΔRH on the bending curvature, keeping the NFC film thickness fixed at 8 μm. **Figure 3**a shows the bending kinetics upon exposing the humidity difference on the film. It shows that for a fixed ΔRH = 40%, a steady-state curvature was obtained within tens of seconds. That a steady state was obtained was confirmed by observing that the curvature was approximately constant for 24 h. For smaller humidity difference values ΔRH, essentially similar observations were made although the steady-state curvature was smaller (see Figure 5a). Figure 3b shows the corresponding kinetics toward a flat state when the humidity stimulus was removed, where the curvature initially quickly decreased in the first 15-20 s, and the ultimately process toward completely flat film was finished eventually in a minute. Similarly, **Figure 4**a shows the development of bending curvature of NFC films of different thicknesses upon keeping a fixed humidity difference ΔRH = 40%. Also, here, the achievement of the steady-state curvature is evident with a fraction of minute, as well as relaxation toward the flat state upon removing the exposed humidity (Figure 4b). As shown in **Figure 5**a, the bending curvature increased gradually from 0.3 to 0.75 cm^{-1} as ΔRH was increased from 10 to 40%, as illustrated for the film of thickness 8 μm. Finally, we investigated the steady-state bending curvatures of the NFC films with different thicknesses while fixing ΔRH at 40% (Figure 5b). Only relatively thin films (i.e., those with thickness less than 20 μm) showed high bending curvature, whereas the film with
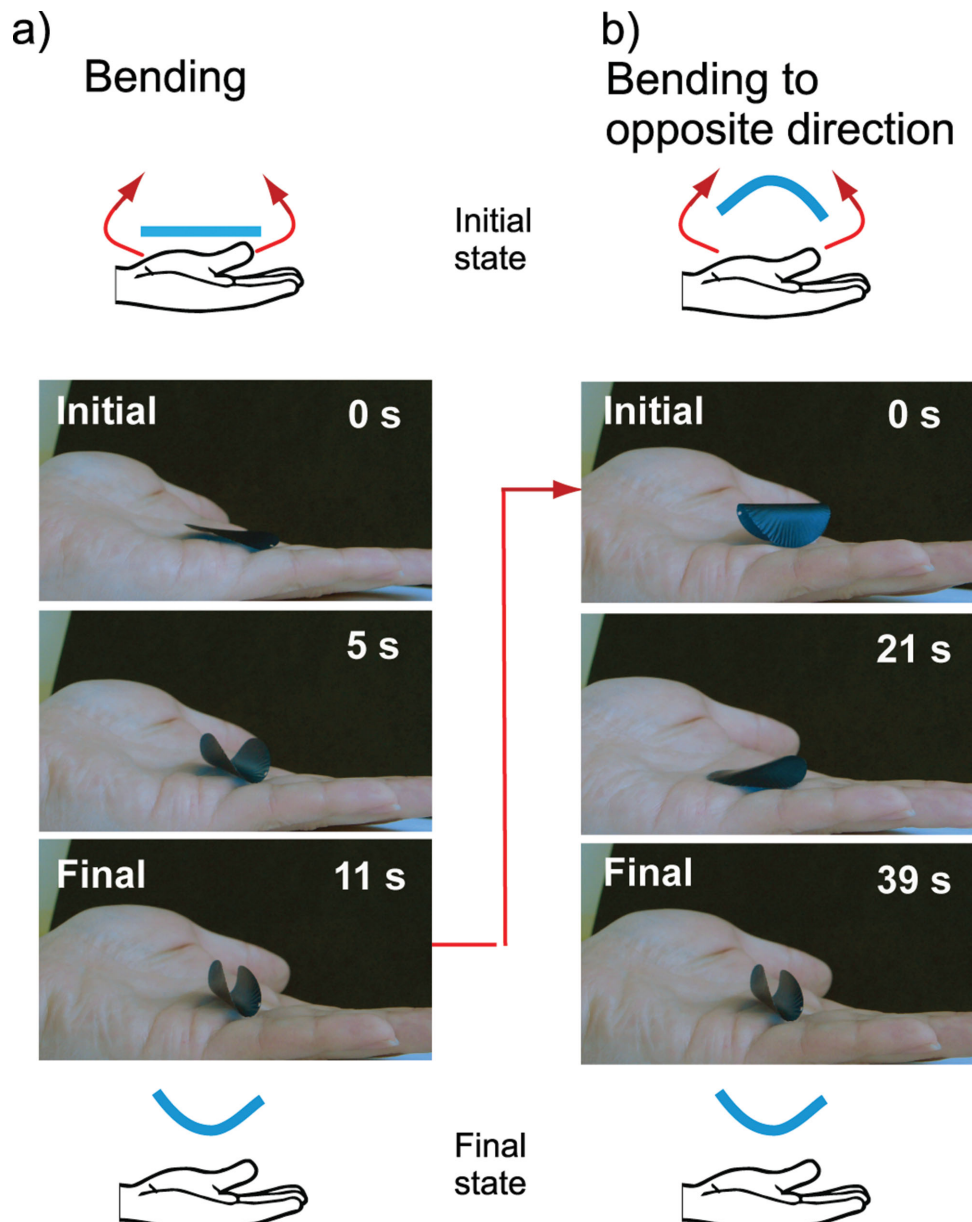
Materials
Views
www.MaterialsViews.com

ADVANCED
MATERIALS
INTERFACES
www.advmatinterfaces.de

Figure 2. Qualitative demonstration of reversible and bidirectional humidity-driven bending of the NFC film. a) The NFC film (dyed blue with methylene blue to promote visualization) bends upward when placed on a hand. b) When the deflected NFC film is turned upside down, it first recovers to its original flat shape and further deflects in the reverse direction. The images are snapshots from Supplementary Movie 1.

a thickness of ≈38 μm showed only moderately small bending of about 0.2 cm^{-1}, and the one with thickness of ≈48 μm exhibited only a minimal curvature. Finally, as a reference, a classic paper sheet of thickness 60 μm and using the humidity of ΔRH = 40% resulted in limited bending during 24 h (Figure S7, Supporting Information). The steady-state bending obtained by exposing the nanocellulose sheets asymmetrically to humidity was unexpected, as previously classic paper sheets were observed to show only transient bending and recovery to flat shape upon placing paper sheets onto liquid water.[18]

Regarding the actuation mechanism, we present arguments that suggest the bending is due to the formation of a bilayer-like structure consisting of asymmetric humidity-swollen and nonswollen layers. First, because of their hygroscopic nature, celluloses are known to swell due to absorbed moisture. Therefore, immediately after exposing the NFC film asymmetrically to water vapors, a thin hydrated swollen surface layer is formed whereas the bulk of the film is still in the equilibrium ambient low humidity state, thus forming a bilayer-like structure. Within a few seconds, the film starts to bend in the direction that is consistent with the volume increase of the hydrated surface layer. Importantly, if the humidity exposure was then stopped after a few seconds, the film recovered its original flat shape in a fraction of a minute. This indicates that the thin swollen layer vanishes, and there remains no asymmetry to drive bending. Indirectly, this shows that the humidity swollen surface layer
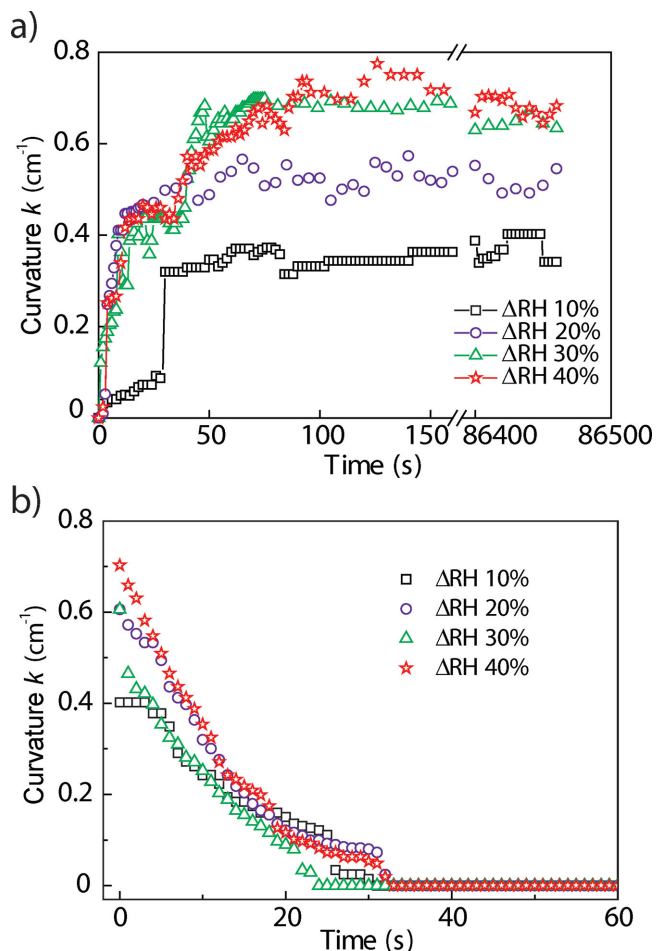
**ADVANCED
MATERIALS
INTERFACES**

www.advmatinterfaces.de

*Materials
Views*

www.MaterialsViews.com

Figure 3. Time dependence of the bending for different humidity values for a fixed film thickness of 8 µm. a) Bending dynamics upon initiating the humidity exposure. b) Relaxation dynamics after removing the humidity exposure. The stepwise scatters in the data reflect on the high sensitivity due to the miniature air flows within the set-up.

Figure 4. Time dependence of the bending for different film thicknesses for a fixed humidity value difference ΔRH = 40%. a) Bending dynamics upon initiating the humidity exposure. b) Relaxation dynamics after removing the humidity exposure.

becomes equilibrated with the ambient low humidity level in a time scale of a minute due to water evaporation. On the other hand, by continued asymmetric exposure to water vapors, the humidity-driven swelling front progresses toward the opposite surface of the film. Also there it is expected that the equilibration of the surface humidity with the lower environmental value takes place, thus leaving effectively a bilayer-like material with a thin nonswollen surface layer. This means that a dynamic balance is acquired, having a swollen layer due to vapor influx and the opposite surface being more dry due to water evaporation. This would explain the steady-state bending.

Although the bending of the NFC films is remarkable, we emphasize that the required swelling to explain the bending is actually very small due to the small film thickness. This can be analyzed by the swelling ratio $\Delta L/L$, where L is the original length of the NFC film and ΔL is the increased length on the swollen side. The swelling ratio can be derived by considering the relationship between the dimensional change and the deflection curvature of the NFC films, and it obeys the following rule (see Supporting Information, Figure S6 and the associated discussion for details)
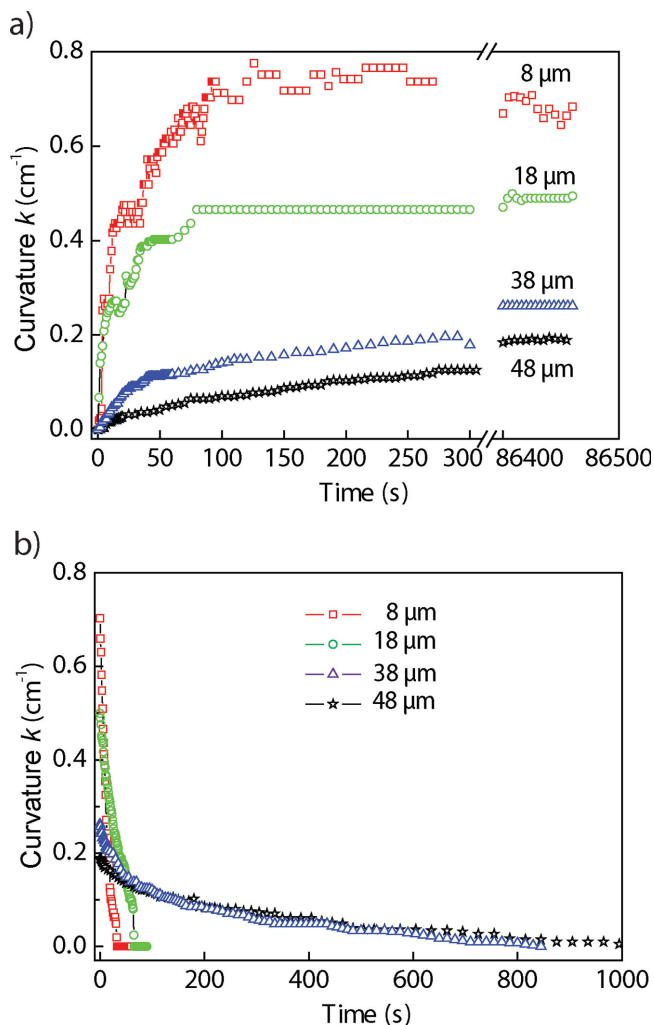
$$\Delta L / L = d * k \qquad (1)$$

where d is the film thickness and k is the deflection curvature of the film. In our experiments, even when ΔRH = 40% (Figure 5b), the swelling ratio of the 8-µm NFC film is estimated to be only about 0.06%; whereas for the 48-µm film, the swelling ratio is about 0.09%. Such small swelling ratios make it not practical to directly demonstrate the volume change of NFC films by conventional microscopy methods in accordance with our experimental observation. From Equation (1), we can also understand the effect of film thickness on its deflection capability. Given a certain swelling ratio, the deflection curvature of a film is inversely proportional to the film thickness. This explains why a thin film is important for sensitive deflection. Use of cellulose nanofibers is important for the remarkable deflection of the films, as it allows more facile bending due to the nanometer lateral diameter in contrast to the thicker paper fibers, which also provide challenges to make very thin films. This reasoning is also supported by our observation
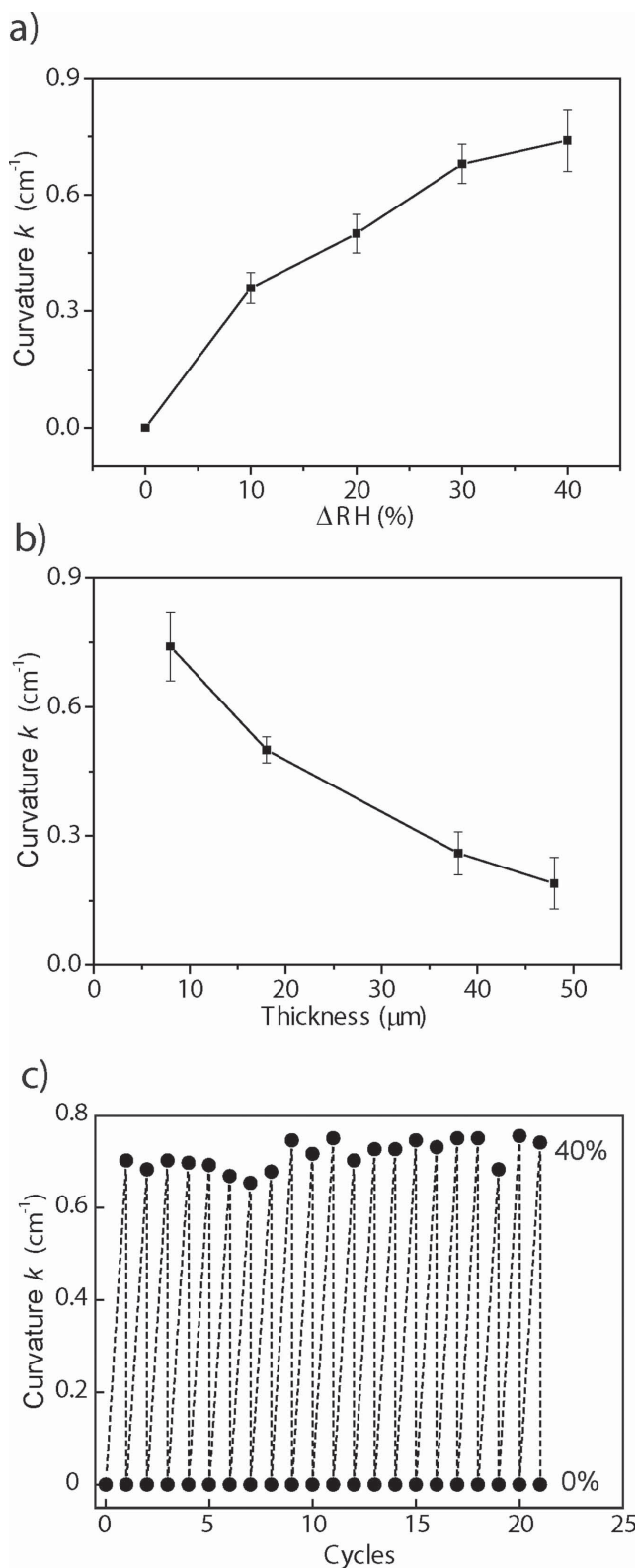
Materials
Views

www.MaterialsViews.com

ADVANCED
MATERIALS
INTERFACES
www.advmatinterfaces.de

a)

b)

c)

Figure 5. a) The steady-state bending curvature as a function of humidity difference (ΔRH) for a film with film thickness of 8 μm. b) The steady-state curvature decreases strongly for increased film thickness at fixed humidity difference $\Delta RH = 40\%$. c) Reversible and repeated deflection of the NFC film (thickness 8 μm) upon cyclic humidity change.

that a classic paper sheet has slow and limited bending upon exposing asymmetrically to water vapor (Figure S7, Supporting Information). Also, if instead of water vapor, liquid water is allowed to penetrate asymmetrically in classic paper sheets, a transient bending is first observed, and thereafter the sheet becomes again flat.[18] These observations suggest that use of cellulose nanofibers allows making thin films and allows sensitive, controlled, and steady-state actuation that leads to conceptually different behavior in comparison to using liquid water and classic paper sheets. Furthermore, the micro-/nanoscale porous structure (Figure S2, Supporting Information, cross-sectional SEM images) of the NFC films may facilitate the moisture imbibition and diffusion within the nanocellulose network when applying the humidity stimulus; it also facilitates the outward diffusion of moisture when removing the humidity stimulus. The microscopic porous structure of the NFC films thus improves their bending and relaxation dynamics performances. Finally, Figure S8 (Supporting Information) shows that to a smaller extent, actuation is driven even by vapor of other volatile polar solvents, such as ethanol and acetone, whereas vapors of nonpolar solvents did not have any effect.

This reversible deflection-recovery process can be repeated for more than 20 cycles without observable fatigue (Figure 5c). The slower recovery rate relative to the deflection process is because of the fact that desorption of moisture is more difficult than its absorption in accordance with the highly hydrophilic and hygroscopic character of the NFC film.

Finally, to qualitatively further demonstrate the high sensitivity for the humidity, the deflection can be even induced at a distance by just approaching a finger toward it, i.e., remotely without direct touching (**Figure 6**, also see Supplementary Movie 2, Supporting Information). When a finger approached the NFC film from the bottom left or bottom right parts, local upward deflection at the corresponding parts readily took place. When the finger approached from the top middle part, the film deflected downward. Therefore, even a very slight and local humidity increase close to the NFC film can create local asymmetric swelling of the film and induce local bending. As a final qualitative example, the shown actuation inspired us to mimic the humidity-dependent curling and blooming glory flower.[20] We prepared a four-petal NFC film "flower" and put it onto a metal mesh. When a water-soaked paper towel was approaching the flower under the mesh, the flower began to fold gradually (**Figure 7**a) due to the upward deflection of the petals. Whereas when the wetted paper towel was withdrawn away, the folded flower would bloom and recover to its original shape through desorption of moisture (Figure 7b). The dynamic folding and blooming process is shown in Supplementary Movie 3 (Supporting Information).

3. Conclusion

We show that sufficiently thin films made of cellulose nanofibers (NFC, MFC) allow water vapor controlled actuation that is sensitive to difference of the humidity levels across the different sides of the film. Unlike the previously reported liquid water driven transient bending of paper sheets, the present concept leads to steady-state bending in a fraction of minute, where

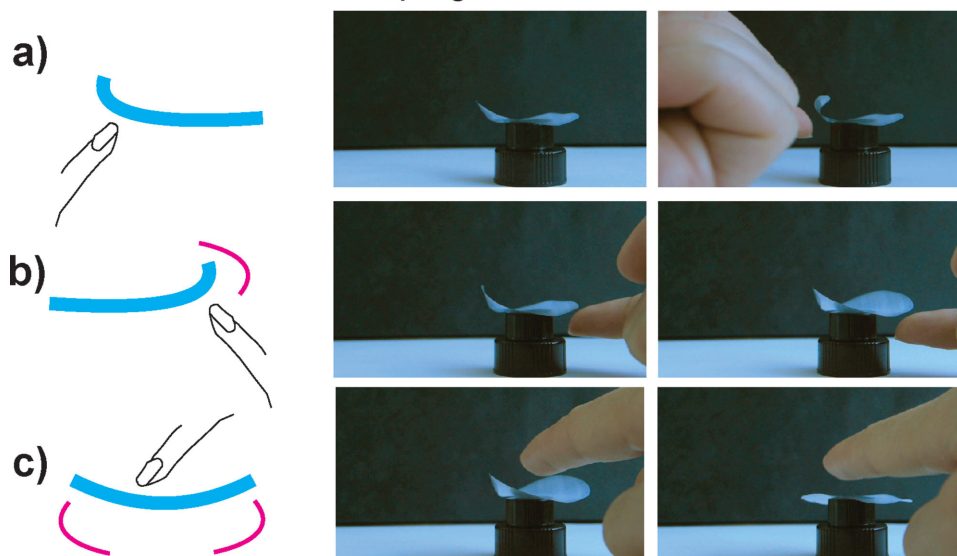## Remote shaping of a nanocellulose film

Figure 6. The sensitivity of the humidity-driven bending is demonstrated here where the bending is induced even by a finger at a distance of a few millimeters, i.e., without direct contact. Upward deflection from the a) left, b) right parts, and downward deflection from c) the central part by approaching a finger toward different parts of the film. The NFC film is placed on the top of a plastic cap. The images are snapshots from Supplementary Movie 2.

the curvature increases based on the humidity. The bending is reversible, directional, and allows cycling, and the extent of the curvature can be controlled by the film thickness. In very thick films, the curvature is not observed. We suggest that the mechanism is based on the formation of a dynamic bilayer-like structure in thin films consisting of the contrast between the water swollen surface and the opposite surface where the water is evaporated. The concept stimulates toward facile and sensitive humidity actuations and sensing, for example, when combining with electroactive and other functional units, as well as devices allowing locomotions.

4. Experimental Section

The nanofibrillated cellulose (NFC) was prepared from an aqueous native birch pulp by first washing to Na+ form using aqueous HCl

(0.1 M) and NaHCO$_3$ (0.005 M). The pH was adjusted to 9 with NaOH and then passed 12 times through a high-pressure homogenizer, which finally formed a hydrogel and the resulted nanofibers have a diameter of ≈9 nm, as described before.[21] The NFC films were prepared by filtration of nanofibrillated cellulose aqueous dispersion (0.1 wt%, diluted from hydrogel), followed by drying under ambient conditions. A millipore membrane (pore size 0.22 µm) was used for filtration. The thickness of NFC films was controlled by adjusting the volume of aqueous dispersion during the filtration process, and a series of NFC films with thicknesses varying from 8 to 48 µm was prepared. Morphology of the NFC film was investigated by field-emission scanning electron microscopy (Zeiss Sigma VP) at 1.5-keV electron energy. All the samples were sputtered with a thin layer of gold/platinum (Emitech K100X) before imaging.

The curvature was calculated as follows

$$\text{Curvature } (k) = \frac{\text{deflection angle} \times \pi \div 180}{L} \tag{2}$$
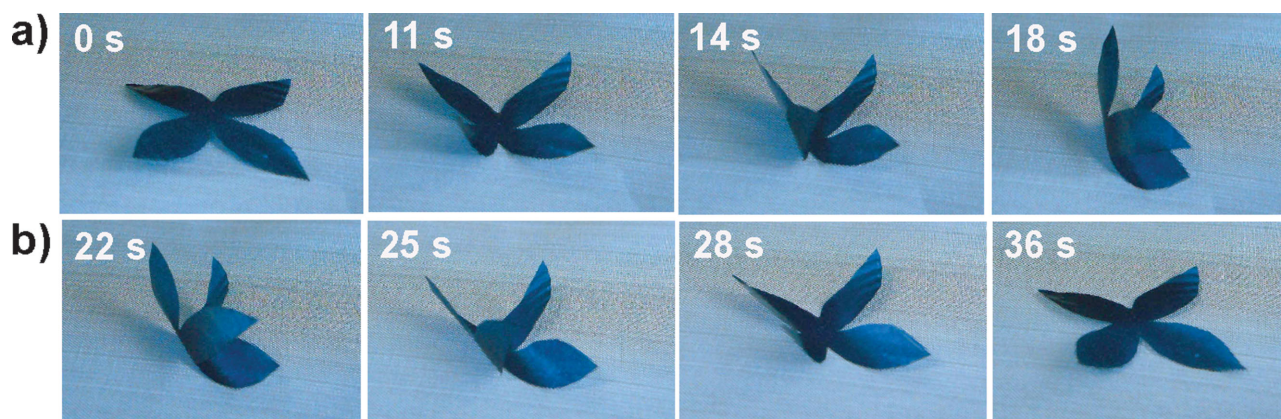

Figure 7. a) The folding and b) blooming of NFC "flower" supported on a metal mesh driven by approaching and withdrawing a water-soaked paper towel under the mesh. The NFC film was dyed blue with methylene blue to aid visualization. The images are snapshots from Supplementary Movie 3.

Materials
Views
www.MaterialsViews.com

ADVANCED
MATERIALS
INTERFACES
www.advmatinterfaces.de

where L is the film-free bending length, as shown in Figure S5 (Supporting Information).

Supporting Information

Supporting Information is available from the Wiley Online Library or from the author.

Acknowledgements

[1] a) P. Fratzl, R. Weinkamer, *Prog. Mater. Sci.* **2007**, *52*, 1263; b) B. Bhushan, *Philos. Trans. R. Soc., A* **2009**, *367*, 1445; c) U. G. K. Wegst, H. Bai, E. Saiz, A. P. Tomsia, R. O. Ritchie, *Nat. Mater.* **2015**, *14*, 23.

[2] a) M. A. Meyers, P.-Y. Chen, A. Y.-M. Lin, Y. Seki, *Prog. Mater. Sci.* **2008**, *53*, 1; b) Z. Tang, N. A. Kotov, S. Magonov, B. Ozturk, *Nat. Mater.* **2003**, *2*, 413; c) E. Munch, M. E. Launey, D. H. Alsem, E. Saiz, A. P. Tomsia, R. O. Ritchie, *Science* **2008**, *322*, 1516; d) L. J. Bonderer, A. R. Studart, L. J. Gauckler, *Science* **2008**, *319*, 1069; e) A. Walther, I. Bjurhager, J.-M. Malho, J. Ruokolainen, J. Pere, L. Berglund, O. Ikkala, *Nano Lett.* **2010**, *10*, 2742.

[3] a) H. Ghiradella, *Appl. Opt.* **1991**, *30*, 3492; b) P. Vukusic, J. R. Sambles, *Nature* **2003**, *424*, 852; c) A. C. Edrington, A. M. Urbas, P. DeRege, C. X. Chen, T. M. Swager, N. Hadjichristidis, M. Xenidou, L. J. Fetters, J. D. Joannopoulos, Y. Fink, E. L. Thomas, *Adv. Mater.* **2002**, *14*, 1853; d) S. Valkama, H. Kosonen, J. Ruokolainen, T. Haatainen, M. Torkkeli, R. Serimaa, G. ten Brinke, O. Ikkala, *Nat. Mater.* **2004**, *3*, 872; e) J. J. Walish, Y. Kang, R. A. Mickiewicz, E. L. Thomas, *Adv. Mater.* **2009**, *21*, 3078; f) K. E. Shopsowitz, H. Qi, W. Y. Hamad, M. J. MacLachlan, *Nature* **2010**, *468*, 422; g) M. Kreysing, R. Pusch, D. Haverkate, M. Landsberger, J. Engelmann, J. Ruiter, C. Mora-Ferrer, E. Ulbricht, J. Grosche, K. Franze, S. Streif, S. Schumacher, F. Makarov, J. Kacza, J. Guck, H. Wolburg, J. K. Bowmaker, G. von der Emde, S. Schuster, H. J. Wagner, A. Reichenbach, M. Francke, *Science* **2012**, *336*, 1700; h) I. B. Burgess, J. Aizenberg, M. Lončar, *Bioinspir. Biomim.* **2013**, *8*, 045004.

[4] a) K. Koch, B. Bhushan, W. Barthlott, *Prog. Mater. Sci.* **2009**, *54*, 137; b) D. Quéré, *Annu. Rev. Mater. Res.* **2008**, *38*, 71; c) T. S. Wong, S. H. Kang, S. K. Y. Tang, E. J. Smythe, B. D. Hatton, A. Grinthal, J. Aizenberg, *Nature* **2011**, *477*, 443; d) T. Verho, L. Sainiemi, V. Jokinen, J. T. Korhonen, C. Bower, K. Franze, S. Franssila, P. Andrew, O. Ikkala, R. H. A. Ras, *Proc. Natl. Acad. Sci. U. S. A.* **2012**, *109*, 10210; e) Y. Tian, B. Su, L. Jiang, *Adv. Mater.* **2014**, *26*, 6872.

[5] a) J. Bath, A. J. Turberfield, *Nat. Nanotechnol.* **2007**, *2*, 275; b) M. Hagiya, A. Konagaya, S. Kobayashi, H. Saito, S. Murata, *Acc. Chem. Res.* **2014**, *47*, 1681.

[6] a) R. Dreyfus, J. Baudry, M. L. Roper, M. Fermigier, H. A. Stone, J. Bibette, *Nature* **2005**, *437*, 862; b) J. X. Zhang, B. Xiang, Q. He, J. Seidel, R. J. Zeches, P. Yu, S. Y. Yang, C. H. Wang, Y. H. Chu, L. W. Martin, A. M. Minor, R. Ramesh, *Nat. Nanotechnol.* **2011**, *6*, 97; c) R. Shankar, T. K. Ghosh, R. J. Spontak, *Adv. Mater.* **2007**, *19*, 2218.

[7] a) S. J. Kim, G. M. Spinks, S. Prosser, P. G. Whitten, G. G. Wallace, S. I. Kim, *Nat. Mater.* **2006**, *5*, 48; b) N. N. Zhang, R. Q. Li, L. Zhang, H. B. Chen, W. C. Wang, Y. Liu, T. Wu, X. D. Wang, W. Wang, Y. Li, Y. Zhao, J. P. Gao, *Soft Matter* **2011**, *7*, 7231; c) S. Naficy, G. M. Spinks, G. G. Wallace, *ACS Appl. Mater. Interfaces* **2014**, *6*, 4109.

[8] a) C. M. Andres, J. Zhu, T. Shyu, C. Flynn, N. A. Kotov, *Langmuir* **2014**, *30*, 5378; b) M. E. Harmon, M. Tang, C. W. Frank, *Polymer* **2003**, *44*, 4547; c) S. Zakharchenko, N. Puretskiy, G. Stoychev, M. Stamm, L. Ionov, *Soft Matter* **2010**, *6*, 2633.

[9] a) Y. L. Yu, M. Nakano, T. Ikeda, *Nature* **2003**, *425*, 145; b) S. Kobatake, S. Takami, H. Muto, T. Ishikawa, M. Irie, *Nature* **2007**, *446*, 778; c) Y. Takashima, S. Hatanaka, M. Otsubo, M. Nakahata, T. Kakuta, A. Hashidzume, H. Yamaguchi, A. Harada, *Nat. Commun.* **2012**, *3*, 1270; d) R. R. Kohlmeyer, J. Chen, *Angew. Chem., Int. Ed.* **2013**, *52*, 9234.

[10] a) S. Park, J. An, J. W. Suk, R. S. Ruoff, *Small* **2010**, *6*, 210; b) Y. Ma, Y. Zhang, B. Wu, W. Sun, Z. Li, J. Sun, *Angew. Chem., Int. Ed.* **2011**, *50*, 6254; c) R. M. Erb, J. S. Sander, R. Grisch, A. R. Studart, *Nat. Commun.* **2013**, *4*, 1712; d) M. Ma, L. Guo, D. G. Anderson, R. Langer, *Science* **2013**, *339*, 186; e) H. H. Cheng, J. Liu, Y. Zhao, C. G. Hu, Z. P. Zhang, N. Chen, L. Jiang, L. T. Qu, *Angew. Chem., Int. Ed.* **2013**, *52*, 10482; f) L. T. de Haan, J. M. N. Verjans, D. J. Broer, C. W. M. Bastiaansen, A. P. H. J. Schenning, *J. Am. Chem. Soc.* **2014**, *136*, 10585.

[11] a) R. H. Baughman, C. X. Cui, A. A. Zakhidov, Z. Iqbal, J. N. Barisci, G. M. Spinks, G. G. Wallace, A. Mazzoldi, D. De Rossi, A. G. Rinzler, O. Jaschinski, S. Roth, M. Kertesz, *Science* **1999**, *284*, 1340; b) E. Smela, *Adv. Mater.* **2003**, *15*, 481; c) J. M. Sansinena, J. B. Gao, H. L. Wang, *Adv. Funct. Mater.* **2003**, *13*, 703; d) X. H. Liu, B. He, Z. P. Wang, H. F. Tang, T. Su, Q. G. Wang, *Sci. Rep.* **2014**, *4*, 6673; e) E. W. H. Jager, E. Smela, O. Inganäs, *Science* **2000**, *290*, 1540; f) L. Kong, W. Chen, *Adv. Mater.* **2014**, *26*, 1025.

[12] a) A. Sidorenko, T. Krupenkin, A. Taylor, P. Fratzl, J. Aizenberg, *Science* **2007**, *315*, 487; b) C. L. van Oosten, C. W. M. Bastiaansen, D. J. Broer, *Nat. Mater.* **2009**, *8*, 677; c) J. V. I. Timonen, C. Johans, K. Kontturi, A. Walther, O. Ikkala, R. H. A. Ras, *ACS Appl. Mater. Interfaces* **2010**, *2*, 2226.

[13] I. Tokarev, M. Orlov, S. Minko, *Adv. Mater.* **2006**, *18*, 2458.

[14] a) I. Burgert, P. Fratzl, *Philos. Trans. R Soc., A* **2009**, *367*, 1541; b) R. Elbaum, L. Zaltzman, I. Burgert, P. Fratzl, *Science* **2007**, *316*, 884; c) Y. Abraham, C. Tamburu, E. Klein, J. W. C. Dunlop, P. Fratzl, U. Raviv, R. Elbaum, *J. R. Soc. Interface* **2012**, *9*, 640; d) S. J. Gerbode, J. R. Puzey, A. G. McCormick, L. Mahadevan, *Science* **2012**, *337*, 1087; e) A. R. Studart, R. M. Erb, *Soft Matter* **2014**, *10*, 1284.

[15] a) C. Dawson, J. F. V. Vincent, A.-M. Rocca, *Nature* **1997**, *390*, 668; b) E. Reyssat, L. Mahadevan, *J. R. Soc. Interface* **2009**, *6*, 951.

[16] S. Timoshenko, *J. Opt. Soc. Am.* **1925**, *11*, 233.

[17] D. Klemm, F. Kramer, S. Moritz, T. Lindström, M. Ankerfors, D. Gray, A. Dorris, *Angew. Chem., Int. Ed.* **2011**, *50*, 5438.

[18] E. Reyssat, L. Mahadevan, *EPL* **2011**, *93*, 54001.

[19] Y. Forterre, *J. Exp. Bot.* **2013**, *64*, 4745.

[20] Y. Ma, J. Sun, *Chem. Mater.* **2009**, *21*, 898.

[21] M. Wang, I. V. Anoshkin, A. G. Nasibulin, J. T. Korhonen, J. Seitsonen, J. Pere, E. I. Kauppinen, R. H. A. Ras, O. Ikkala, *Adv. Mater.* **2013**, *25*, 2428.